PHYSICAL REVIEW D **95,** 045006 (2017)

Leading and subleading UV divergences in scattering amplitudes for $D=8$ $\mathcal{N}=1$ SYM theory in all loops

D. I. Kazakov[1,2,3] and D. E. Vlasenko[4]

[1]*Bogoliubov Laboratory of Theoretical Physics, Joint Institute for Nuclear Research, Dubna, Russia*
[2]*Alikhanov Institute for Theoretical and Experimental Physics, Moscow, Russia*
[3]*Moscow Institute of Physics and Technology, Dolgoprudny, Russia*
[4]*Department of Physics, South Federal State University, Rostov-Don, Russia*

(Received 17 May 2016; published 21 February 2017)

We consider the leading and subleading UV divergences for the four-point on-shell scattering amplitudes in $D=8$ $\mathcal{N}=1$ supersymmetric Yang-Mills theory in the planar limit. This theory belongs to the class of maximally supersymmetric gauge theories and presumably possesses distinguished properties beyond perturbation theory. We obtain the recursive relations that allow one to get the leading and subleading divergences in all loops in a pure algebraic way staring from the one loop (for the leading poles) and two loop (for the subleading ones) diagrams. As a particular example where the recursive relations have a simple form we consider the ladder type diagrams. The all-loop summation of the leading and subleading divergences is performed with the help of the differential equations which are the generalization of the RG equations for nonrenormalizable theories. They have explicit solutions for the ladder type diagrams. We discuss the properties of the obtained solutions and interpretation of the results.

DOI: 10.1103/PhysRevD.95.045006

I. INTRODUCTION

In the last decade there has been considerable activity on the calculation of the amplitudes in maximally supersymmetric Yang-Mills theories (SYM) [1,2] and maximally supersymmetric gravity [3]. Gauge and gravity SUSY theories in $D=4$ such as the $\mathcal{N}=4$ SYM and $\mathcal{N}=8$ SUGRA are the most important examples. These theories are believed to possess several remarkable properties, among which are total or partial cancellation of UV divergences, factorization of higher loop corrections, and possible integrability. The success of factorization leading to the BDS ansatz [1] for the amplitudes in $D=4$ $\mathcal{N}=4$ SYM stimulated similar activity in other models and dimensions. Many magnificent insights in the structure of amplitudes (the S-matrix) of gauge theories in various dimensions (for review see, for example, [4]) were obtained.

In recent papers [5,6] we considered the leading UV divergences of the on-shell scattering amplitudes in maximally supersymmetric SYM theories in $D=6$ ($\mathcal{N}=2$ SUSY), $D=8$ ($\mathcal{N}=1$ SUSY), and $D=10$ ($\mathcal{N}=1$ SUSY) dimensions. In these theories the on-shell amplitudes are IR finite and the only divergences are the UV ones. Since the gauge coupling g^2 in D dimensions has dimension $[4-D]$, all these theories are nonrenormalizable.

Applying first the color decomposition of the amplitudes we are left with the partial amplitudes. Within the spinor-helicity formalism [2], the tree-level partial amplitudes have a relatively simple universal form and always factorize so that the ratio of the loop corrections to the tree-level expression can be expressed in terms of scalar master integrals. For the four-point amplitude this is shown schematically in Fig. 1.

The on-shell four-point amplitude depends on the Mandelstam variables s, t, and u with the condition $s+t+u=0$. Within the dimensional regularization (dimensional reduction) the UV divergences manifest themselves as the pole terms with the numerators being the polynomials over the kinematical variables. This expansion has a universal form in any dimension including the combinatoric factors that contain the coupling constant and the powers of s and t. The dependence on particular value of D comes from the integration inside the loops.

In D dimensions the first UV divergences start from $L=6/(D-4)$ loops. Consequently in $D=6$ they start

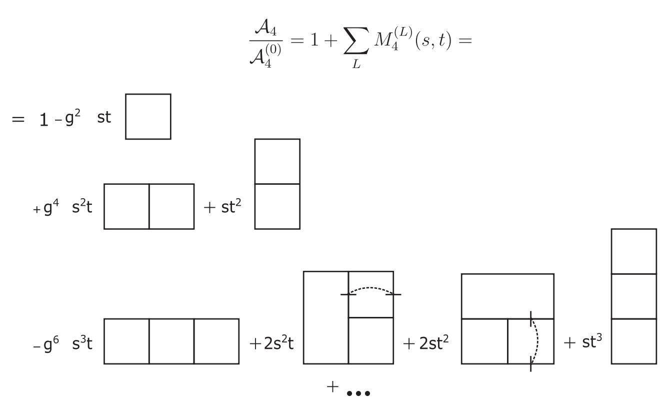

FIG. 1. The universal expansion for the four-point scattering amplitude in SYM theories in terms of master integrals. The connected strokes on the lines mean the square of the flowing momentum.

 © 2017 American Physical Society

from 3 loops. In $D = 8$ and $D = 10$, though the one-loop case is somewhat special, they start already at one loop. In [6] we considered the leading divergences in all of these cases. Here, we concentrate on the $D = 8$ case since the loop order is less than in the $D = 6$ case and the numerators are not so complex as in the $D = 10$ case. Contrary to [6], we go beyond the leading divergences and consider the subleading ones in order to understand the tendency and to check whether the subleading terms change the situation regarding the renormalization of the theory in all loops.

II. $\mathcal{R}'$ OPERATION AND POLE EQUATIONS IN THE LEADING AND SUBLEADING ORDER

Any local quantum field theory has a remarkable property that after performing the incomplete $\mathcal{R}$ operation, the so-called $\mathcal{R}'$ operation, the remaining UV divergences are always local. Let us briefly recall the main notions of the $\mathcal{R}$ operation [7,8]. Being applied to any Green function Γ (or any particular graph G) it subtracts all the UV divergences including those of divergent subgraphs and leaves the finite expression. The use of the $\mathcal{R}$ operation is equivalent to addition of the counter terms to the initial Lagrangian. The $\mathcal{R}$ operation can be written in terms of subtraction operators in the factorized form

$$\mathcal{R}G = \prod_{\gamma}(1 - M_{\gamma})G, \tag{1}$$

where the subtraction operator M_{γ} subtracts the UV divergence of a given subgraph γ and the product goes over all divergent subgraphs including the graph itself.

It is useful to define also the incomplete $\mathcal{R}$ operation denoted by $\mathcal{R}'$ which subtracts only the subdivergences of the graph G. The full $\mathcal{R}$ operation is then defined as

$$\mathcal{R}G = (1 - \mathcal{K})\mathcal{R}'G, \tag{2}$$

where $\mathcal{K}$ is an operator that singles out the singular part of the graph (for the minimal subtraction scheme the operator $\mathcal{K}$ singles out the $1/\epsilon^n$ terms). The $\mathcal{K}\mathcal{R}'G$ is the counterterm corresponding to the graph G. Each counter term contains only the superficial divergence and is *local* in coordinate space (in our case it must be a polynomial of external momenta).

The $\mathcal{R}'$ operation for any graph G can be defined by the forest formula, but for our calculations it is more convenient to use the recursive definition via the $\mathcal{R}'$ operation for divergent subgraphs (for details and examples see chapter 3 in [9]):

$$\mathcal{R}'G = \left(1 - \sum_{\gamma}\mathcal{K}R'_{\gamma} + \sum_{\gamma,\gamma'}\mathcal{K}R'_{\gamma}\mathcal{K}R'_{\gamma'} - \cdots\right)G. \tag{3}$$

The sum goes over all 1PI, UV-divergent subgraphs of the given diagram and the multiple sums include only the nonintersecting subgraphs.

When applying this formula to the diagrams at hand one finds that for the n-loop diagram the $\mathcal{R}'$ operation results in the series of terms (we consider the leading and subleading poles)

$$\begin{aligned}\mathcal{R}'G_n = {}& \frac{\mathcal{A}_n^{(n)}(\mu^2)^{n\epsilon}}{\epsilon^n} + \frac{\mathcal{A}_{n-1}^{(n)}(\mu^2)^{(n-1)\epsilon}}{\epsilon^n} + \cdots + \frac{\mathcal{A}_1^{(n)}(\mu^2)^{\epsilon}}{\epsilon^n} \\ & + \frac{\mathcal{B}_n^{(n)}(\mu^2)^{n\epsilon}}{\epsilon^{n-1}} + \frac{\mathcal{B}_{n-1}^{(n)}(\mu^2)^{(n-1)\epsilon}}{\epsilon^{n-1}} + \cdots + \frac{\mathcal{B}_1^{(n)}(\mu^2)^{\epsilon}}{\epsilon^{n-1}} \\ & + \text{lower order terms},\end{aligned} \tag{4}$$

where the terms like $\frac{\mathcal{A}_k^{(n)}(\mu^2)^{k\epsilon}}{\epsilon^n}$ and $\frac{\mathcal{B}_k^{(n)}(\mu^2)^{k\epsilon}}{\epsilon^{n-1}}$ come from the k-loop graph which survives after subtraction of the $(n-k)$-loop counterterm. The full expression (4) has to be local, i.e. should not contain terms like $(\log\mu)^k/\epsilon^m$ for all k, $m > 0$ while being expanded over ϵ. (For simplicity hereafter we put $\mu^2 \equiv \mu$.) This requirement gives us $n-1$ equations for the coefficients $\mathcal{A}_i^{(n)}$ and $n-2$ equations for the coefficients $\mathcal{B}_i^{(n)}$. Solving them in favor of the one- and two-loop graphs one gets

$$\mathcal{A}_n^{(n)} = (-1)^{n+1}\frac{\mathcal{A}_1^{(n)}}{n}, \tag{5}$$

$$\mathcal{B}_n^{(n)} = (-1)^n\left(\frac{2}{n}\mathcal{B}_2^{(n)} + \frac{n-2}{n}\mathcal{B}_1^{(n)}\right). \tag{6}$$

It is also useful to have analogous expressions for the $\mathcal{K}R'$ terms equal to

$$\mathcal{K}R'G_n = \sum_{k=1}^{n}\left(\frac{\mathcal{A}_k^{(n)}}{\epsilon^n} + \frac{\mathcal{B}_k^{(n)}}{\epsilon^{n-1}}\right) \equiv \frac{\mathcal{A}_n^{(n)'}}{\epsilon^n} + \frac{\mathcal{B}_n^{(n)'}}{\epsilon^{n-1}}. \tag{7}$$

One has, respectively,

$$\mathcal{A}_n^{(n)'} = (-1)^{n+1}\mathcal{A}_n^{(n)} = \frac{\mathcal{A}_1^{(n)}}{n}, \tag{8}$$

$$\mathcal{B}_n^{(n)'} = \left(\frac{2}{n(n-1)}\mathcal{B}_2^{(n)} + \frac{2}{n}\mathcal{B}_1^{(n)}\right). \tag{9}$$

This means that performing the $\mathcal{R}'$ operation one can take care only of the one loop diagrams surviving after contraction and get the desired leading pole term via Eq. (5) and add the two-loop diagrams to get the subleading pole from Eq. (6). This observation drastically simplifies the calculation of the leading and subleading poles. Moreover, it follows from Eqs. (5) and (6) that, just as in renormalizable theories, the leading poles are essentially governed by

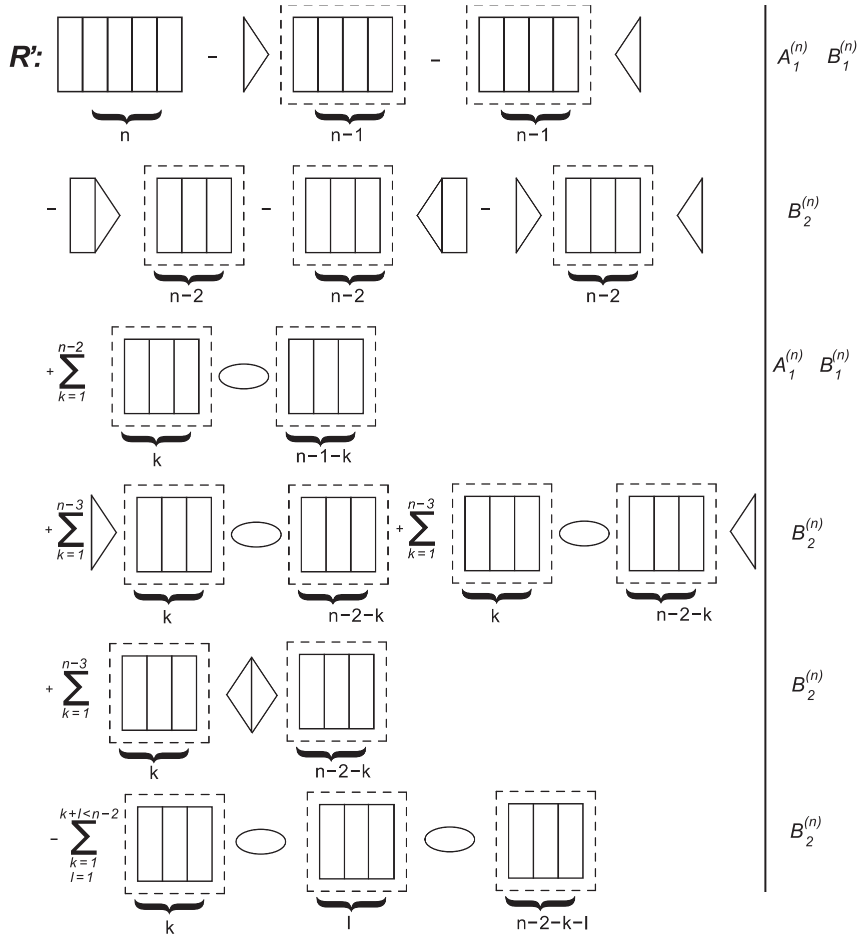

FIG. 2. The application of the $\mathcal{R}'$ operation to the ladder type diagrams. At the right it is shown to which term of expansion (4) it corresponds to.

the one-loop diagrams and can be deduced from them in all loops pure algebraically, while to know the subleading poles in all loops one needs to know the subleading pole of the two-loop diagrams. We demonstrate below how this procedure works in practice and obtain explicit formulas for the leading and subleading poles in all loops.

III. THE LEADING POLES IN ALL LOOPS

We start with the leading poles and consider as a simplest example the $\mathcal{R}'$ operation applied to the ladder type diagrams (see Fig. 2).

To calculate the contribution to $\mathcal{A}_1^{(n)}$ one has to calculate the poles of the one-loop diagrams in the first and the third row. For $\mathcal{B}_1^{(n)}$ one needs the constant part of these one-loop graphs and for $\mathcal{B}_2^{(n)}$ one needs the leading and subleading poles of the two-loop diagrams from the second and fourth row.

We first concentrate on the leading poles. For the s-channel ladder type diagram they depend only on s so that $\mathcal{A}_n^{(n)} = s^{n-1}A_n$. Calculating the needed one-loop diagrams and substituting them into Eq. (5) one gets the recursion relation

$$nA_n = -\frac{2}{4!}A_{n-1} + \frac{2}{5!}\sum_{k=1}^{n-2} A_k A_{n-1-k}, \qquad n \geq 3 \tag{10}$$

with $A_1 = 1/3!$. Starting from this value one can calculate any A_n though explicit solution of the recursion relation (10) is not straightforward.

However, since we actually need the sum of the series we perform the summation multiplying both sides of Eq. (10) by $(-z)^{n-1}$, where $z = \frac{g^2}{\epsilon}$ and take the sum from 3 to infinity

$$\sum_{n=3}^{\infty} nA_n(-z)^{n-1} = -\frac{2}{4!}\sum_{n=3}^{\infty} A_{n-1}(-z)^{n-1} + \frac{2}{5!}\sum_{n=3}^{\infty}\sum_{k=1}^{n-2} A_k(-z)^k A_{n-1-k}(-z)^{n-1-k}. \tag{11}$$

Denoting now the sum $\sum_{n=m}^{\infty} A_n(-z)^n$ by Σ_m and performing the interchange of the order of summation in the nonlinear term we get

$$-\frac{d}{dz}\Sigma_3 = -\frac{2}{4!}\Sigma_2 + \frac{2}{5!}\Sigma_1\Sigma_1. \tag{12}$$

Having in mind that

$$\Sigma_3 = \Sigma_1 + A_1 z - A_2 z^2, \qquad \Sigma_2 = \Sigma_1 + A_1 z,$$
$$A_1 = \frac{1}{3!}, \qquad A_2 = -\frac{1}{3!4!},$$

one finally gets the equation for $\Sigma_A \equiv \Sigma_1$

$$\frac{d}{dz}\Sigma_A = -\frac{1}{3!} + \frac{2}{4!}\Sigma_A - \frac{2}{5!}\Sigma_A^2. \tag{13}$$

The solution to this equation is

$$\Sigma_A(z) = -\sqrt{5/3}\frac{4\tan(z/(8\sqrt{15}))}{1-\tan(z/(8\sqrt{15}))\sqrt{5/3}} = \sqrt{10}\frac{\sin(z/(8\sqrt{15}))}{\sin(z/(8\sqrt{15})-z_0)}, \tag{14}$$

where $z_0 = \arcsin(\sqrt{3/8})$. The expansion of $\tan z$ contains the Bernoulli numbers

$$\tan z = \sum_{n=1}^{\infty}(-1)^{n-1}\frac{2^{2n}(2^{2n}-1)B_{2n}}{(2n)!}z^{2n-1}.$$

Being substituted into Eq. (14) it gives

$$\Sigma_A(z) = -(z/6 + z^2/144 + z^3/2880 + 7z^4/414720 + \cdots). \tag{15}$$

Note that taking into account the combinatoric factors the dimensionless variable z is given by $z = \frac{g^2 s^2}{\epsilon}$. This series reproduces the ladder type diagrams in all orders. The same is obviously true for the t-channel ladder diagram with the replacement $s \leftrightarrow t$. The function Σ_A given by Eq. (14) has an infinite sequence of simple poles and thus has no limit when $z \to \infty$ i.e., $\epsilon \to 0$.

The recursion relation (10) can be generalized to include all diagrams contributing to the four-point amplitude. It was obtained in [6] and we present here a short summary. It is worth mentioning that not all the four-point diagrams contribute to the leading pole but only those which contain the subgraphs of each previous order. These diagrams can be constructed with the help of the so-called rung rule, described in [6]. But even among them there are zero contributions which come from the diagrams that are reduced to the two-point functions after shrinking the subgraphs when performing the $\mathcal{R}'$ operation.

To present the recursion relation for the full set of relevant diagrams we note that they can be divided into two classes: the s-channel and the t-channel ones and the total contribution is the sum of them. The singularity of G_n is a polynomial in s and t. When calculating $\mathcal{A}_1^{(n)}$ like in Fig. 2 for the s-channel diagrams, s stands as a constant factor while t from $\mathcal{K}R'G_{n-1}$ contains the integration momentum over the last loop. The same is true for the t-channel diagrams with the replacement $s \leftrightarrow t$.

As a result, when using the $\mathcal{R}'$ operation one is left with the remaining triangle and bubble one-loop diagrams shown in the first and the third rows of Fig. 2. Substituting the explicit form of s and t and integrating over the triangle and the bubble with the help of the Feynman parameters one gets the desired recursion relation. Note that for the bubble term when integrating over the loop on both sides one has functions of s and t. Replacing t by t' one should have in mind that on the left $t' = (l-p_1)^2$ and on the right $t' = (l+p_4^2)$, where l is the integration momentum. This means that after integration one gets mixed terms like $g^{\mu\nu}p_1^\mu p_4^\nu$. They give rise to the double sum in the second term of the equation. Eventually one has

$$\begin{aligned} nS_n(s,t) = {} & -2s^2\int_0^1 dx\int_0^x dy\, y(1-x)(S_{n-1}(s,t') + T_{n-1}(s,t'))|_{t'=tx+yu} \\ & + s^4\int_0^1 dx x^2(1-x)^2\sum_{k=1}^{n-2}\sum_{p=0}^{2k-2}\frac{1}{p!(p+2)!}\frac{d^p}{dt'^p}(S_k(s,t') + T_k(s,t')) \\ & \times\frac{d^p}{dt'^p}(S_{n-1-k}(s,t') + T_{n-1-k}(s,t'))|_{t'=-sx}(tsx(1-x))^p, \end{aligned} \tag{16}$$

where $t' = tx + uy$, $u = -t - s$, and $S_1 = \frac{1}{12}$, $T_1 = \frac{1}{12}$.

Here we denote by $S_n(s,t)$ and $T_n(s,t)$ the sum of all contributions in the nth order of PT in s and t channels, respectively.

The same recursive relation is valid for the t-channel diagrams with the obvious replacement $s \leftrightarrow t$. Due to the $s-t$ symmetry of the amplitude, one should have $T_n(s,t) = S_n(t,s)$. The coefficient $\mathcal{A}_n^{(n)}(s,t)$ of the nth order pole is the sum

$$\mathcal{A}_n^{(n)}(s,t) = S_n(s,t) + T_n(s,t).$$

Equation (16) can be summed the same way as in the ladder case (11). Multiplying both sides by $(-z)^{n-1}$ and summing up over n from 3 to infinity one gets

$$\frac{d}{dz}\Sigma_3(s,t,z) = 2s^2\int_0^1 dx\int_0^x dyy(1-x)(\Sigma_2(s,t',z)+\Sigma_2(t',s,z)|_{t'=tx+yu} \\ - s^4\int_0^1 dxx^2(1-x)^2\sum_{p=0}^{\infty}\frac{1}{p!(p+2)!}\left(\frac{d^p}{dt'^p}(\Sigma_1(s,t',z)+\Sigma_1(t',s,z)|_{t'=-sx}\right)^2(tsx(1-x))^p. \quad (17)$$

Using now that

$$\Sigma_3(s,t,z) = \Sigma_1(s,t,z) - S_2(s,t)z^2 + S_1(s,t)z, \qquad \Sigma_2(s,t,z) = \Sigma_1(s,t,z) + S_1(s,t)z,$$
$$\frac{d}{dz}\Sigma_3(s,t,z) = \frac{d}{dz}\Sigma_1(s,t,z) - 2S_2(s,t)z + S_1(s,t), \qquad 2S_2(s,t) = 2s^2\int(S_1(s,t')+S_1(t',s))$$

and making notation $\Sigma(s,t,z) = \Sigma_1(s,t,z)$ one finally obtains

$$\frac{d}{dz}\Sigma(s,t,z) = -\frac{1}{12} + 2s^2\int_0^1 dx\int_0^x dy\, y(1-x)(\Sigma(s,t',z)+\Sigma(t',s,z))|_{t'=tx+yu} \\ - s^4\int_0^1 dxx^2(1-x)^2\sum_{p=0}^{\infty}\frac{1}{p!(p+2)!}\left(\frac{d^p}{dt'^p}(\Sigma(s,t',z)+\Sigma(t',s,z))|_{t'=-sx}\right)^2(tsx(1-x))^p. \quad (18)$$

The same equation with the replacement $s \leftrightarrow t$ can be derived for $\Sigma(t,s,z)$.

Contrary to the ladder case (13), the solution of Eq. (18) is not straightforward and is difficult to analyze.

IV. THE SUBLEADING POLES IN ALL LOOPS: THE LADDER DIAGRAMS

We now turn to the subleading pole. As an example we again consider the ladder diagrams. Contrary to the leading case, here the input is defined not only by the one loop diagrams, but by the two-loop ones as well. The subleading pole of the two-loop box has to be explicitly evaluated; it cannot be deduced from the recursion relations as it follows from Eq. (6). Explicit evaluation gives

$$\text{Box} = \frac{1}{3!\epsilon}, \qquad \text{Double Box} = -\frac{1}{3!4!}\left(\frac{s}{\epsilon^2}+\frac{27}{4}\frac{s}{\epsilon}+\frac{1}{6}\frac{t}{\epsilon}\right). \quad (19)$$

Together with the other one- and two-loop diagrams evaluated up to the subleading order we obtain the expressions for $\mathcal{B}_1^{(n)}$ and $\mathcal{B}_2^{(n)}$ from the diagrams of Fig. 2. The evaluation of some two-loop diagrams is quite a cumbersome task; for instance, the rhombus one has been calculated using the integration by parts technique [10]. Hereafter we use the notation

$$\mathcal{A}_n^{(n)} = s^{n-1}A_n, \qquad \mathcal{A}_n^{(n)'} = s^{n-1}A'_n, \qquad \mathcal{B}_n^{(n)} = s^{n-1}B_{sn} + s^{n-2}tB_{tn}, \qquad \mathcal{B}_n^{(n)'} = s^{n-1}B'_{sn} + s^{n-2}tB'_{tn}.$$

We get

$$\mathcal{B}_1^{(n)} = -A'_{n-1}s^{n-2}\left(-\frac{s}{4!}\right)\frac{19}{6}2 - B'_{sn-1}s^{n-2}\left(-\frac{s}{4!}\right)2 - B'_{tn-1}s^{n-3}\left(-\frac{s}{5!}\right)(t-2s)2 \\ + \sum_{k=1}^{n-2}A'_k s^{k-1}A'_{n-1-k}s^{n-2-k}\left(\frac{2s^2}{5!}\right)\frac{46}{15} \\ + \sum_{k=1}^{n-2}A'_k s^{k-1}B'_{sn-1-k}s^{n-2-k}\left(\frac{2s^2}{5!}\right)2 + \sum_{k=1}^{n-2}A'_k s^{k-1}B'_{tn-1-k}s^{n-3-k}\left(\frac{-s^3}{5!}\right)2, \quad (20)$$

$$\begin{aligned}
\mathcal{B}_2^{(n)} = & -A'_{n-2}s^{n-3}\left(\frac{s^2}{3!4!}\right)\frac{5063}{2400}2 - B'_{sn-2}s^{n-3}\left(\frac{s^2}{3!4!}\right)\frac{13}{40}2 - B'_{tn-1}s^{n-4}\left(\frac{s^2}{5!5!}\right)\frac{t-32s}{2}2 \\
& - A'_{n-2}s^{n-3}\left(-\frac{s}{4!}\right)\left(-\frac{s}{4!}\frac{19}{6}\right)2 - B'_{sn-2}s^{n-3}\left(-\frac{s}{4!}\right)\left(-\frac{s}{4!}\right) - B'_{tn-2}s^{n-4}\left(-\frac{s^2}{5!5!}\right)(12s-t) \\
& + \sum_{k=1}^{n-3} A'_k s^{k-1} A'_{n-2-k} s^{n-3-k}\left(-\frac{s^3}{5!4!}\right)\frac{938}{15} \\
& + \sum_{k=1}^{n-3} A'_k s^{k-1} B'_{sn-2-k} s^{n-3-k}\left(-\frac{s^3}{5!2}\right) + \sum_{k=1}^{n-3} A'_k s^{k-1} B'_{tn-2-k} s^{n-4-k}\left(\frac{442s^4}{5!5!12}\right) \\
& - \sum_{k,l=1}^{n-k+l<n-2} A'_k s^{k-1} A'_l s^{l-1} A'_{n-2-k-l} s^{n-3-k-l}\left(\frac{2s^2}{5!}\right)\left(\frac{2s^2}{5!}\right)\frac{46}{15}2 \\
& - \sum_{k,l=1}^{n-k+l<n-2} A'_k s^{k-1} A'_l s^{l-1} B'_{sn-2-k-l} s^{n-3-k-l}\left(\frac{2s^2}{5!}\right)\left(\frac{2s^2}{5!}\right)3 \\
& - \sum_{k,l=1}^{n-k+l<n-2} A'_k s^{k-1} A'_l s^{l-1} B'_{tn-2-k-l} s^{n-4-k-l}\left(\frac{2s^2}{5!}\right)\left(-\frac{s^3}{5!}\right)2 \\
& - \sum_{k,l=1}^{n-k+l<n-2} A'_k s^{k-1} B'_{tl} s^{l-2} A'_{n-2-k-l} s^{n-3-k-l}\left(\frac{-2s^5}{5!5!}\right). \qquad (21)
\end{aligned}$$

These expressions it their turn allow us to get the desired recursion relations for the primed coefficients using Eq. (9)

$$B'_{tn} = -\frac{2}{n(n-1)}B'_{tn-2}\frac{10}{5!5!} + \frac{2}{n}B'_{tn-1}\frac{2}{5!}, \qquad (22)$$

$$\begin{aligned}
B'_{sn} = & \frac{2}{n(n-1)}\left[-A'_{n-2}\frac{2321}{5!5!2} - B'_{sn-2}\frac{18}{4!5!} + B'_{tn-2}\frac{44}{5!5!}\right. \\
& - \sum_{k=1}^{n-3} A'_k A'_{n-2-k}\frac{938}{4!5!15} - \sum_{k=1}^{n-3} A'_k B'_{sn-2-k}\frac{1}{5!2} + \sum_{k=1}^{n-3} A'_k B'_{tn-2-k}\frac{442}{5!5!12} \\
& - \sum_{k,l=1}^{n-k+l<n-2} A'_k A'_l A'_{n-2-k-l}\frac{8}{5!5!}\frac{46}{15} - \sum_{k,l=1}^{n-k+l<n-2} A'_k A'_l B'_{sn-2-k-l}\frac{12}{5!5!} \\
& \left. + \sum_{k,l=1}^{n-k+l<n-2} A'_k A'_l B'_{tn-2-k-l}\frac{4}{5!5!} + \sum_{k,l=1}^{n-k+l<n-2} B'_k A'_l A'_{sn-2-k-l}\frac{2}{5!5!}\right] \\
& + \frac{2}{n}\left[A'_{n-1}\frac{19}{34!} + B'_{sn-1}\frac{2}{4!} - B'_{tn-1}\frac{4}{5!}\right. \\
& \left. + \sum_{k=1}^{n-2} A'_k A'_{n-1-k}\frac{2}{5!}\frac{46}{15} + \sum_{k=1}^{n-2} A'_k B'_{sn-1-k}\frac{4}{5!} - \sum_{k=1}^{n-2} A'_k B'_{tn-1-k}\frac{2}{5!}\right]. \qquad (23)
\end{aligned}$$

One can write down the corresponding relations for the unprimed coefficients in terms of the primed ones. For B_{tn} it looks like

$$B_{tn} = (-1)^n\left[-\frac{2}{n}B'_{tn-2}\frac{10}{5!5!} + \frac{n-2}{n}B'_{tn-1}\frac{2}{5!}\right] \qquad (24)$$

and similar for B_{sn}. Starting from the initial values

$$B'_{s1} = B'_{t1} = 0, \qquad B'_{s2} = -\frac{1}{3!4!}\frac{5}{12}, \qquad B'_{t2} = -\frac{1}{3!4!}\frac{1}{6},$$
$$B_{s2} = -\frac{1}{3!4!}\frac{27}{4}, \qquad B_{t2} = -\frac{1}{3!4!}\frac{1}{6}, \qquad A_1 = \frac{1}{3!}$$

they allow one to calculate the corresponding coefficients at any order. One can write down a simple *Mathematica* routine to evaluate them purely algebraically (see *Mathematica* file in Supplemental Material [11]).

The last step is to sum the series. In order to do it we again write down the differential equation for the sum. Let us begin with B'_{tn}. Multiplying Eq. (22) by z^{n-2} and taking the sum from 3 to infinity we get the differential equation for $\Sigma'_{tB} \equiv \Sigma'_{tB2} = \sum_2^\infty z^n B'_{tn}$

$$\frac{d^2\Sigma'_{tB}(z)}{dz^2} - \frac{1}{30}\frac{d\Sigma'_{tB}(z)}{dz} + \frac{\Sigma'_{tB}(z)}{720} = -\frac{1}{432} \tag{25}$$

in full analogy with Eq. (13). Having in mind the boundary conditions $\Sigma'_{tB}(0) = \frac{d\Sigma'_{tB}(0)}{dz} = 0$, one gets the solution

$$\Sigma'_{tB}(z) = \frac{5}{6}[e^{z/60}(-\sin[z/30] + 2\cos[z/30]) - 2]. \tag{26}$$

One can write down the equation for the unprimed $\Sigma_{tB} \equiv \Sigma_{tB2} = \sum_2^\infty (-z)^n B_{tn}$. It follows from Eq. (24) and has the form

$$\frac{d\Sigma_{tB}(z)}{dz} = \frac{1}{60} z \frac{d\Sigma'_{tB}(z)}{dz} - \frac{\Sigma'_{tB}(z)}{60} - z\frac{\Sigma'_{tB}(z)}{720} - \frac{z}{432}. \tag{27}$$

Solving this equation having in mind Eq. (26) one gets

$$\Sigma_{tB}(z) = -\frac{1}{36}[60 + z + e^{z/60}(-(60+z)\cos[z/30] - 2(-15+z)\sin[z/30])]. \tag{28}$$

It is more difficult to get the closed expressions for Σ'_{sB} and Σ_{sB}. Again we start with the primed coefficients. Taking Eq. (23) as input, multiplying it by z^{n-2} and taking the sum from 3 to infinity, we get the following differential equation for $\Sigma'_{sB} \equiv \Sigma'_{sB2} = \sum_2^\infty z^n B'_{sn}$:

$$\frac{d^2\Sigma'_{sB}(z)}{dz^2} + f_1(z)\frac{d\Sigma'_{sB}(z)}{dz} + f_2(z)\Sigma'_{sB}(z) = f_3(z), \tag{29}$$

where

$$f_1(z) = -\frac{1}{6} + \frac{\Sigma_A}{15},$$
$$f_2(z) = \frac{1}{80} - \frac{\Sigma_A}{120} + \frac{\Sigma_A^2}{600} + \frac{1}{15}\frac{d\Sigma_A}{dz},$$
$$f_3(z) = \frac{2321}{5!5!2}\Sigma_A + \frac{11}{1800}\Sigma'_{tB} - \frac{469}{5!90}\Sigma_A^2 - \frac{442}{5!5!6}\Sigma_A\Sigma'_{tB} + \frac{23}{6750}\Sigma_A^3 + \frac{1}{1200}\Sigma_A^2\Sigma'_{tB} - \frac{19}{36}\frac{d\Sigma_A}{dz} - \frac{1}{15}\frac{d\Sigma'_{tB}}{dz} + \frac{23}{225}\frac{d\Sigma_A^2}{dz} + \frac{1}{30}\frac{d(\Sigma_A\Sigma'_{tB})}{dz} - \frac{3}{32}.$$

This is a general Riccati equation. Surprisingly the solution can be found by a simple substitution. We discuss it in the next section.

Similarly to Eq. (27) one can write down the equation for $\Sigma_{sB} \equiv \Sigma_{sB2} = \sum_2^\infty (-z)^n B_{sn}$. It can be solved in terms of Σ'_{sB} and Σ'_{tB} in a straightforward way:

$$\Sigma_{sB} = \left(z\frac{d}{dz} - 1\right)\Sigma'_{sB} - z\left(-\frac{19}{72}\Sigma_A + \frac{1}{12}\Sigma'_{sB} - \frac{1}{30}\Sigma'_{tB} + \frac{23}{450}\Sigma_A^2 - \frac{1}{30}\Sigma_A\Sigma'_{sB} + \frac{1}{60}\Sigma_A\Sigma'_{tB}\right). \tag{30}$$

V. PROPERTIES OF THE SOLUTIONS

We discuss here some properties of solutions of Eqs. (29) and (30). Equation (29) is a linear inhomogeneous second-order differential equation. Surprisingly enough it and can be simplified making the substitution $\Sigma'_{sB}(z) = \frac{d\Sigma_A}{dz}u(z)$. Then, using Eq. (13), it is reduced to a simple one for the function $u(z)$:

$$u''(z)\frac{d\Sigma_A}{dz} = f_3(z), \tag{31}$$

which is trivially solvable in quadratures

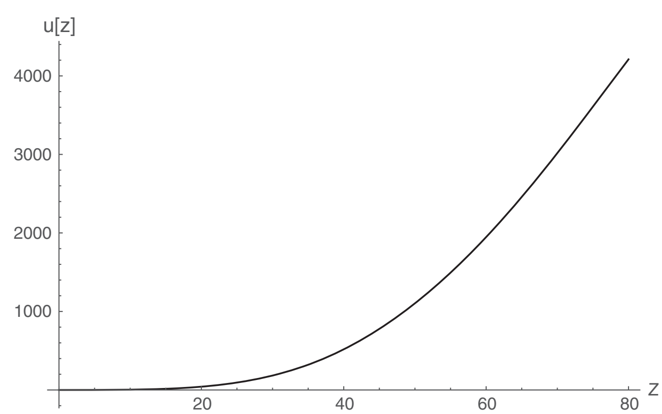

FIG. 3. The behavior of $u(z)$ evaluated numerically.

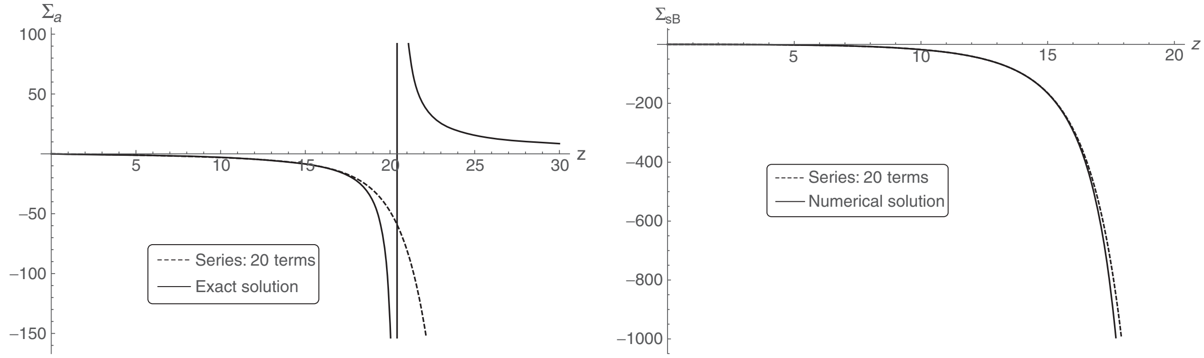

FIG. 4. Comparison of the exact solution with the perturbation series including 20 terms for Σ_A (left) and for Σ_{sB} (right). The solid line is the exact (numerical) solution and the dotted line is the PT series summation result.

$$u(z) = \int_0^z dy \int_0^y dx \frac{f_3(x)}{\Sigma'_A(x)}. \tag{32}$$

The numerical integration demonstrates that $u(z)$ is a smooth function (see Fig. 3) which increases $\mathrm{Exp}[z/60]$ just like Σ'_{tB} and has no poles so that the singularities of $\Sigma'_{sB}(z)$ come only from Σ'_A.

To get the function Σ_{sB} one has to substitute the functions Σ'_{sB} and Σ'_{tB} into Eq. (30). One can do it numerically. The singularities of the obtained function are governed by the leading term Σ_A and its derivative. Consider them in more detail.

The leading divergences are given by Σ_A (14). It is a singular periodic function which has zeroes at $z/8/\sqrt{15} = \pi n$ and first order poles at $z/8/\sqrt{15} = \arcsin\sqrt{3/8} + \pi n$. Summation of perturbative expansion (15) gives a satisfactory approximation between zero and the first pole at $z \approx 20.42$; however, it fails to go beyond as can be seen in Fig. 4 (left).

Turning to subleading divergences given by Σ_{sB} (30) we notice that Eq. (30) contains the singular functions Σ_A and Σ'_{sB} which possess the poles at the same points. Thus, we expect that the function Σ_{sB} is a singular function of the same kind and also contains poles. Hence, the numerical solution is due to be valid in the interval between zero and the first pole. In the same interval one can also perform a summation of perturbation series generated with the help of the code mentioned above [11]. We present in Fig. 4 (right) the result of numerical solution of Eqs. (29) and (30) together with the perturbation theory series taking into account 20 terms of expansion.

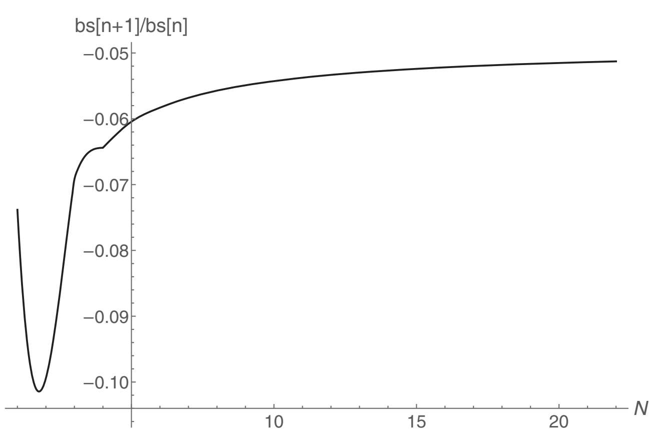

FIG. 5. The ratio of the coefficients $bs[n]$: $R = bs[n+1]/bs[n]$.

There are two main conclusions that one can make analyzing these plots. First of all, the PT works pretty well in the interval between zero and the first pole and the more terms that are taken into account the better. In the case when we know the exact solution as for Σ_A we can convince ourselves that the series is indeed convergent. In the case of Σ_{sB} we check it numerically plotting the ratio of the coefficients $bs[n+1]/bs[n]$ (see Fig. 5).

One can see that after some first orders it goes to the limit equal to ≈ -0.05 which indicates the geometric progression type behavior. Thus, the perturbation series seems to be convergent independently of the sign alternation.

The second conclusion concerns the singularity of the obtained functions. The total contribution of the leading and subleading divergences for the ladder type diagrams in all orders can be written as

$$\Sigma_{\mathrm{Ladder}} = \Sigma_A(z) + \epsilon\left(\Sigma_{sB}(z) + \frac{t}{s}\Sigma_{tB}(z)\right) + \cdots,$$
$$z \equiv \frac{g^2 s^2}{\epsilon}. \tag{33}$$

From the analytical solution for $\Sigma_A(z)$ (14) and Σ_{tB} (28) we see that while Σ_A has an infinite sequence of poles, Σ_{tB} exponentially grows although slower than Σ_A. At the same time, from the numerical solution for Σ_{sB} it follows that it apparently inherits the singularities of Σ_A and does not cancel them. Thus, one can conclude that the subleading divergences do not change the pattern of the leading ones.

VI. DISCUSSION

Summarizing the presented results concerning the subleading divergences one should stress once more that, as it follows from the general theorems, the all-loop terms are governed by the two-loop subleading contributions. We have presented explicit formulas confirming this statement for the ladder case and have demonstrated how the higher terms of PT can be calculated from the lower ones via pure algebraic recursive relations. The corresponding equations for the sum of all-loop contributions (25), (27), (29), (30) generalize the usual renormalization group relations for the pole terms for the case of nonrenormalizable interactions.

To make everything explicit and transparent we chose the set of the ladder type diagrams and performed the summation of the leading and subleading divergences in all loops. Even this task happened to be quite complicated and we were bound to use numerical methods. However, the result of summation of subleading divergences does not lead to any qualitative difference from the leading terms. All the main features of the leading divergences were left untouched.

As for the total set of diagrams, already the leading divergences described by Eq. (18) are difficult to analyze. Following the same lines one can construct an analogous equation for the subleading divergences but it will be even more complicated. The key question here is whether the account of all diagrams will improve the behavior of the laddrer type diagrams and remove the infinite sequence of poles or not. The more general question is to make sense of nonrenormalizable interactions and to interpret the obtained results. Does the limit when $\epsilon \to 0$ exists or not? Does the infinite sequence of poles, if it survives, have anything to do with the infinite number of bound states like in a string theory or not [12]? We leave the analysis of these questions to further publications.

ACKNOWLEDGMENTS

The authors are grateful to M. Kompaniets for a numerical check of the 3- and 4-loop ladder type diagrams and to L. Bork for numerous useful discussions. Financial support from RFBR Grants No. 14-02-00494 and No. 16-32-00737 is acknowledged.

[1] Z. Bern, L. J. Dixon, and V. A. Smirnov, Iteration of planar amplitudes in maximally supersymmetric Yang-Mills theory at three loops and beyond, Phys. Rev. D **72**, 085001 (2005); Z. Bern, M. Czakon, L. Dixon, D. A. Kosower, and V. A. Smirnov, Four-loop planar amplitude and cusp anomalous dimension in maximally supersymmetric Yang-Mills theory., Phys. Rev. D **75**, 085010 (2007); L. J. Dixon, J. M. Drummond, C. Duhr, and J. Pennington, The four-loop remainder function and multi-Regge behavior at NNLLA in planar $\mathcal{N} = 4$ super-Yang-Mills theory, J. High Energy Phys. 06 (2014) 116.

[2] Z. Bern, J. J. Carrasco, L. J. Dixon, M. R. Douglas, M. von Hippel, and H. Johansson, $D = 5$ maximally supersymmetric Yang-Mills theory diverges at six loops, Phys. Rev. D **87**, 025018 (2013).

[3] Z. Bern, J. J. M. Carrasco, and H. Johansson, Progress on ultraviolet finiteness of supergravity, Subnuclear series **46**, 251 (2011); Z. Bern, J. J. Carrasco, L. Dixon, H. Johansson, and R. Roiban, Amplitudes and ultraviolet behavior of $N = 8$ supergravity, Fortschr. Phys. **59**, 561 (2011); H. Elvang, D. Z. Freedman, and M. Kiermaier, SUSY Ward identities, Superamplitudes, and Counterterms, J. Phys. A **44**, 454009 (2011).

[4] Z. Bern, L. J. Dixon, and D. A. Kosower, On-shell methods in perturbative QCD, Ann. Phys. (Berlin) **322**, 1587 (2007); R. Britto, Loop amplitudes in gauge theories: Modern analytic approaches, J. Phys. A **44**, 454006 (2011); Z. Bern and Yu-tin Huang, Basics of generalized unitarity, J. Phys. A **44**, 454003 (2011); H. Elvang and Yu-tin Huang, Scattering amplitudes, arXiv: 1308.1697v1.

[5] L. V. Bork, D. I. Kazakov, and D. E. Vlasenko, Challenges of $D = 6$ $N = (1, 1)$ SYM theory, Phys. Lett. B **734**, 111 (2014).

[6] L. V. Bork, D. I. Kazakov, M. V. Kompaniets, D. M. Tolkachev, and D. E. Vlasenko, Divergences in maximal supersymmetric Yang-Mills theories in diverse dimensions, J. High Energy Phys. 11 (2015) 059.

[7] N. N. Bogolyubov and D. V. Shirkov, *Introduction to the Theory of Quantized Fields* (Nauka, Moscow, 1957, 1973, 1976, 1984) [*Introduction to the Theory of Quantized Fields*, 3rd ed. (Wiley, New York, 1980)].

[8] O. I. Zavyalov, *Renormalized Feynman Diagrams* (Nauka, Moscow, 1979) [*Renormalized Quantum Field Theory* (Kluwer, Dordrecht, 1990)].

[9] A. N. Vasilev, *Quantum Field Renormalization Group in Critical Behavior Theory and Stochastic Dynamics* (Petersburg Inst. Nucl. Phys., St. Petersburg State University, 1998) [*The Field Theoretic Renormalization Group in Critical Behavior Theory and Stochastic Dynamics* (Chapman & Hall/CRC, Boca Raton, 2004)].

[10] K. G. Chetyrkin and F. V. Tkachov, Integration by parts: An algorithm to calculate 4-loop β-function, Nucl. Phys. **B192**, 159 (1981); D. I. Kazakov, Teor. Mat. Fiz. **58**, 343 (1984) [Calculation of Feynman diagrams by the Uniqueness method, Theor. Math. Phys. **58**, 223 (1984)].

[11] See Supplemental Material at http://link.aps.org/supplemental/10.1103/PhysRevD.95.045006 for generating code of UV coefficients for any loop order as well as the formulas for its summation are presented.

[12] M. B. Green, J. H. Shwarz, and L. Brink, $N = 4$ Yang-Mills and $N = 8$ supergravity as limits of string theories, Nucl. Phys. **B198**, 474 (1982); S. Sannan, Gravity as the limit of the type II superstring theory, Phys. Rev. D **34**, 1749 (1986).